Migration of Bubbles in Ice Under a Temperature Gradient

N. S. STEHLE

U.S. Naval Civil Engineering Laboratory, Port Hueneme, California, U.S.A.

Abstract

A laboratory investigation of the migration velocity of air bubbles and vapor figures was carried out at the Naval Civil Engineering Laboratory, Port Hueneme, California, U. S. A., in order to test the theory of the migration of fluid inclusions under a temperature gradient, to verify Nakaya's investigations of the migration of vapor figures under a temperature gradient, and to investigate the physical characteristics of bubbles in polar ice under a temperature gradient, with the purpose of obtaining insight into the physical mechanisms governing the behavior of bubbles in glaciers and of brine pocket migration in sea ice.

The migration velocities of vapor figures measured in this investigation agreed with those of Nakaya, but his theoretical formula for the migration velocities of vapor figures had to be modified to take into account the effect of internal air pressure and figure shape. The observed velocities of vapor figures and air bubbles supported the theoretical velocity calculations. It was determined that temperature at the bubble, bubble shape, which changed during migration, and the air pressure in the bubble, which varied among bubbles, markedly affected the velocity. In addition to changing shape during migration, the bubbles gradually filled with frost. The effect of frost on the velocity, and the reason for its formation could not be completely explained.

I. Introduction

Most temperate glacier ice contains numerous bubbles of trapped air (Flint, 1947, p. 15). With time and pressure, firn on the glacier changes from loose granules having a porosity of nearly 50% to ice in which the original pore space of the firn occurs as bubbles of trapped air, and sometimes, water (Bader, 1950, p. 443; Nutt, 1959, p. 57). Often, however, these bubbles are not uniformly distributed, but are segregated into alternating discontinuous gradational layers of clear and bubbly ice ranging from 1 to 100 cm in thickness. This layering is a secondary metamorphic structure that, in places, transects the primary sedimentary stratification of the ice. It is, therefore, termed foliation, although it is not foliation in the usual sense because individual large ice crystals commonly extend through several layers of clear and bubbly ice (Allen and others, 1960, p. 606). It is believed that this bubble foliation deforms passively with the glacier movement; that is, that the bubbles do not move significantly relative to the enclosing ice (Kamb, 1959, p. 1893; Fisher, 1962, p. 56; Bader, 1950, p. 450; Allen and others, 1960, pp. 606, 607).

Clear ice also occurs in temperate valley glaciers as more extensive layers, of apparently different origin, adjacent to the side walls, where they may be 0.1 m thick (Seligman, 1949, p. 260) and along the glacier bed, where they may be 0.3 (McCall, 1952, p. 128) to 24 m thick (Kamb and Shreve, 1963, p. 103).

Bubble-free ice has also been found in otherwise bubbly polar glacier ice (glaciers at a temperature below freezing). Rigsby (1955, pp. 3, 4) observed bubble foliation in ice on the Nuna Ramp and on the Moltke Glacier, Greenland; Rausch (1958, p. 28) in the Tuto ice tunnel, Greenland; and Atherton (1963, p. 554) on Lyngbrae, Greenland, observed numerous closely spaced bubble-free and bubbly ice layers which probably represented foliation.

Outcrops of clear ice ranging from 675 m long and 100 m wide (Zumberge and others, 1960, p. 7) to 25,000 m long and 8,000 m wide (Crary and Wilson, 1961, p. 1046), possibly analogous to the clear ice along temperate glacier margins, have been observed on polar glaciers near rock outcrops.

The occurrence in both temperate and polar glaciers of bubble-free ice in large lenses and in layers of foliation has been attributed variously to saturation of firn by summer melt water (Fisher, 1962, p. 58; Allen and others, 1960, p. 606; King and Lewis, 1961, pp. 919, 929; Zumberge and others, 1960, p. 91; Rausch, 1958, p. 28), to pressure melting at isolated points along a closed crevasse (Atherton, 1963, p. 554), to shearing and recrystallization (Bader, 1950, p. 450) and to horizontal compression (Crary and Wilson, 1961, p. 1046).

To understand the occurrences of bubble-foliation and large lenses of bubble-free ice in both polar and temperate glaciers, it is necessary to understand how bubbles in ice behave under the appropriate conditions of stress and temperature. Foliation might not, for example, lie passively within the glacier. In addition, a concentration of bubbles might affect the behavior of nearby bubbles so that they tend to join the concentration. Also, the process by which bubble-free layers in foliation are formed may not be the same as that by which the large bubble-free lenses are created. More generally, the problem of bubble-free ice is part of the broader glaciological problem of the behavior of all fluid inclusions in ice, which comprise not only air bubbles but also vapor figures and brine pockets.

Vapor figures. Solar radiation induces internal melting at nuclei in ice, producing essentially planar, hexagonal cavities, or Tyndall figures, perpendicular to the crystallographic *c*-axis (hexagonal system), generally spaced about 0.5 mm apart, each containing water and a bubble of vapor. The presence of the vapor bubble is due to the difference in specific volume between ice and water (Nakaya, 1956, p. 23). If the ice is subjected to a temperature gradient during refreezing of the Tyndall figure, the vapor bubble may become isolated from the water as it freezes (Nakaya, 1956, p. 15). The water-vapor bubble which remains after freezing of the Tyndall figure is termed a vapor figure. It appears as a thin mirror-like hexagonal disk in the (0001)-plane of the crystal (Nakaya, 1956, p. 1). The vapor figure is saturated with water vapor, and usually contains no air. However, in a few vapor figures, Nakaya (1956, pp. 13, 29) found an air pressure of 0.5×10^{-7} atm or greater; in one, he found a pressure of 0.01 atm.

In a vapor figure subjected to a temperature gradient perpendicular to the plane of the figure, ice sublimates from the warm side of the figure and condenses on the cold side; thus, the figure migrates toward the higher temperature. In calculating the velocity of migration of vapor figures, Nakaya assumed that the thin flat vapor figure does not disturb the flow of heat, and that conduction across the figure is negligible with respect

to convection by vapor. On these assumptions, Nakaya (1956, p. 32) derived the formula

$$V = \frac{K}{\rho \lambda}, \tag{1}$$

for the migration velocity of a vapor figure under a unit temperature gradient. In this formula λ is the heat of sublimation ($=680\ \mathrm{cal \cdot gm^{-1}}$), ρ is the density ($=0.92\ \mathrm{gm \cdot cm^{-3}}$), and K is the thermal conductivity ($=4\times10^{-3}\ \mathrm{cal \cdot sec^{-1} \cdot cm^{-1} \cdot {}^{\circ}C^{-1}}$) of the ice, all of which Nakaya (1956, p. 33) considered to be independent of temperature. The thermal conductivity (Dorsey, 1940, p. 482) and the heat of sublimation (Dorsey, 1940, p. 616; Barnes,

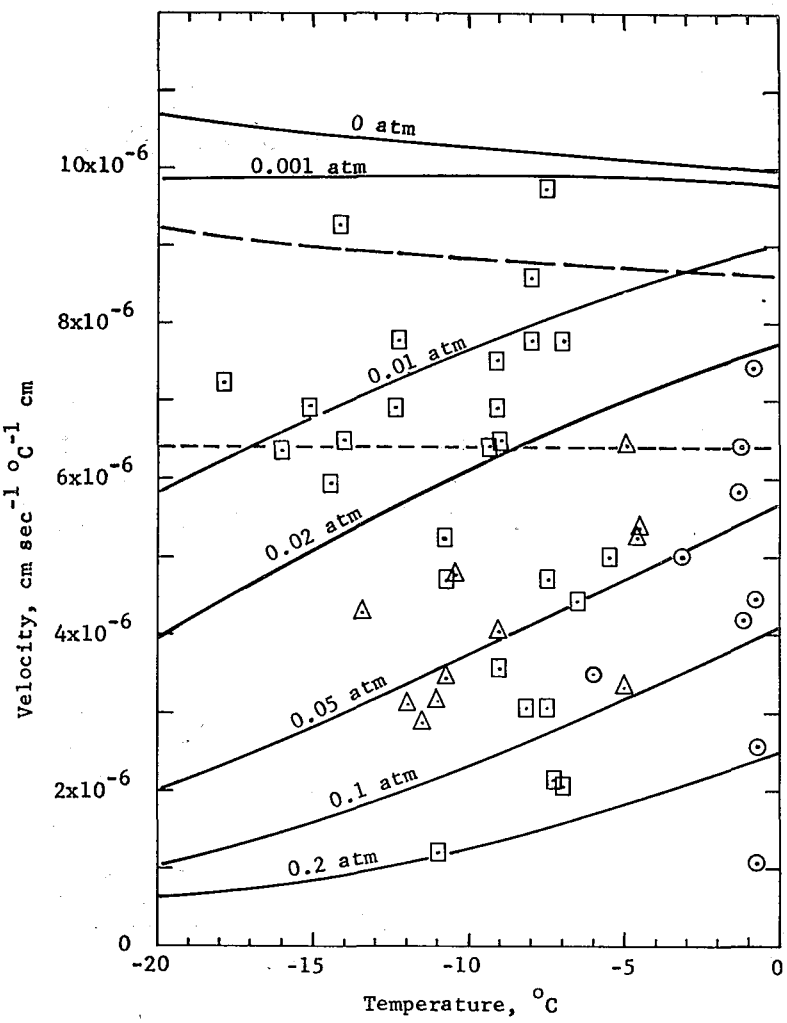

Fig. 1. Theoretical and observed vapor figure velocities

1928, p. 31), however, are significantly temperature dependent. Curves of V using both Nakaya's values and the revised values in eq. (1) are shown in Fig. 1.

Utilizing single crystals of glacier ice under a temperature gradient perpendicular to the plane of the vapor figure, Nakaya (1956, p. 33) obtained migration of the figure toward the warmer side at rates up to 6.4×10^{-6} cm·sec^{-1}·°C^{-1}·cm under temperature gradients ranging from 0.36 to 2.65 °C·cm^{-1} at mean temperatures ranging from −5.5 to −16.1°C. These results are plotted in Fig. 1. The vapor figure became thinner and wider as it migrated. When it became very thin (no dimensions were given), it migrated more slowly (Nakaya, 1956, p. 33).

When air was introduced into the figure, migration ceased or slowed to less than 0.14 cm·sec^{-1}·°C^{-1}·cm. Nakaya (1956, pp. 55, 58, 60) attributed this decrease in velocity to the formation of planar hoarfrost crystals which were caused by the presence of air molecules. Upon examination, he found that the planes of these crystals were parallel to the plane of the vapor figure.

Brine pocket migration. Sea water crystallizes as parallel tabular nearly pure ice platelets parallel to the (0001)-plane and spaced about 0.5 mm apart. Salts and air from the sea water concentrate in brine pockets which lie in the (0001)-planes between the ice platelets. Weeks (1958, p. 97) likens these brine pockets to Tyndall figures because of their similar occurrence perpendicular to the crystallographic c-axis.

Natural sea ice that is several months old contains less salt than newly frozen sea ice; that which has survived through the summer generally produces potable water on melting (Malmgren, 1927, p. 6). Whitman (1926, p. 127) attributes this decrease in salinity to migration of the brine under the temperature gradient present in a floating ice sheet. According to the phase diagram for a brine solution, at any temperature where ice and brine can coexist, the brine solution will have a definite composition at equilibrium. If the temperature of the solution increases, some ice will melt and dilute the solution until it has attained the equilibrium concentration. Therefore, a brine pocket which is under a temperature gradient tends to migrate toward the higher temperatures by melting on the warm side and freezing on the cold side (Whitman, 1926, pp. 127, 128). Although Whitman did not actually measure the rate of migration of individual brine pockets, he did subject samples of ice frozen from sea water to vertical temperature gradients of both signs. In both cases, the brine content of the ice increased at the warm end and decreased at the cold end (Whitman, 1926, p. 131).

Kingery and Goodnow (1963, pp. 243, 244) measured the velocity of individual brine pockets in a 1.5°C·cm^{-1} gradient (−5 to −20°C). Velocities varied from 0 to 8.5×10^{-7} cm·sec^{-1}, with the mean being 2.2×10^{-7} cm·sec^{-1}, the median being 1.2×10^{-7} cm·sec^{-1}, and the mode being about 1.5×10^{-7} cm·sec^{-1}. The brine pockets were at different temperatures, which may account for some of the variation in velocity (p. 244), since Hoekstra and others (1965, p.5038) concluded from similar experiments that for brine pockets very near the same temperature, the velocity was proportional to temperature gradient.

Kingery and Goodnow (1963, p. 244) suggest two limiting factors affecting velocity. One is the rate at which the salt can diffuse across the brine pocket. For a sodium chloride brine, they calculated an average velocity of a brine pocket at about 9.7×10^{-7} cm·sec^{-1}, which was four times more than the average observed velocity and slightly

more than the maximum observed. The second limiting factor is the rate of heat flow required for melting and recrystallization of the ice. In rough calculations, however, Kingery and Goodnow (1963, p. 244) showed this factor to be limiting only at a velocity of 3.7×10^{-4} cm·sec^{-1}, several orders of magnitude larger than observed. Hoekstra and others (1965, p. 5038) found that experimental values of velocity were consistently less than values based on a diffusion theory, but that changes in velocity with temperature were similar; in addition, they found that the migration velocity was not affected by its relation to crystal orientation. From these experiments, they concluded that brine pocket migration is consistent with a theory of migration based on diffusion as the dominant limiting mechanism, and that melting and freezing is not a dominant rate-controlling mechanism. According to Shreve's theory of bubble migration (1964, personal communication), the limiting factors are the diffusion rate of water molecules through the brine pocket and the rate of change of the brine concentration with temperature, both of which are temperature sensitive.

Theory. The theoretical velocities of various shapes of bubbles in ice have been calculated by Shreve (1964, personal communication) assuming a linear temperature gradient at large distances from the bubble. The general equation has the form

$$\frac{1}{V}=\left(1-A\right)\frac{\rho\lambda}{K}+A\,\frac{\rho}{DC}\,, \tag{2}$$

where A is a dimensionless factor dependent upon the shape of the bubble, ρ is the density (Butkovich, 1955, p. 4), K is the thermal conductivity (Dorsey, 1940, p. 482), and λ is the heat of sublimation of the ice (Dorsey, 1940, p. 616; Barnes, 1928, p. 31), C is the rate of change with temperature of the concentration of water vapor in saturated air (National Research Council, 1926, V. 3, p. 210) and D is the diffusion constant at the temperature of the bubble (National Research Council, 1926, V. 5, p. 62).

Two classes of bubble shapes were considered: oblate and prolate spheroids with the axis of rotational symmetry parallel to the temperature gradient, and elliptical cylinders with one semiaxis parallel and the cylinder axis perpendicular to the gradient. Spherical bubbles, thin disks, and circular cylindrical holes are important special cases of these more general shapes.

For oblate spheroidal bubbles with the axis parallel to the gradient

$$A=\zeta\left[(1+\zeta^2)\cot^{-1}\zeta-\zeta\right],$$

where $\zeta^2=a^2/(b^2-a^2)$, in which a is the polar radius, and b is the equatorial radius; whereas, for prolate spheroidal bubbles with the axis parallel to the gradient

$$A=\eta\left[(1-\eta^2)\coth^{-1}\eta+\eta\right],$$

where

$$\eta^2=a^2/(a^2-b^2)\,.$$

For elliptical cylindrical holes,

$$A=\frac{m}{m+n}\,,$$

in which m and n are the semiaxes parallel and perpendicular to the gradient, respectively.

The factor $\rho\lambda/K$ in eq. (2) is related to the rate at which heat is supplied to vaporize the ice on the warm side and is removed to refreeze the vapor on the cold side of the bubble. The factor ρ/DC is related to the rate at which the vapor diffuses across the bubble. A vapor figure, which is a bubble containing little or no air, is effectively a better conductor of heat than the ice so that the lines of heat flow converge on it; hence, the velocity of migration is limited by the rate at which heat can flow from the ice. The presence of air in the bubble causes it to be effectively a poorer conductor of heat than the ice so that the heat flow is partially diverted around the bubble and the velocity of migration decreases.

In most vapor figures, the air pressure is so low that the diffusion constant D is extremely large, and eq. (2) becomes approximately

$$\frac{1}{V} = \left(1-A\right)\frac{\rho\lambda}{K}.$$

For an infinitely thin disk $a/b=0$, hence, $A=0$, so that eq. (1), the formula of Nakaya (1956, p.32), applies. It would also apply to an air bubble of the same shape. For many vapor figures, however, a/b is as great as 0.1 (Nakaya, 1956, pp. 31, 32) for which $A=0.137$.

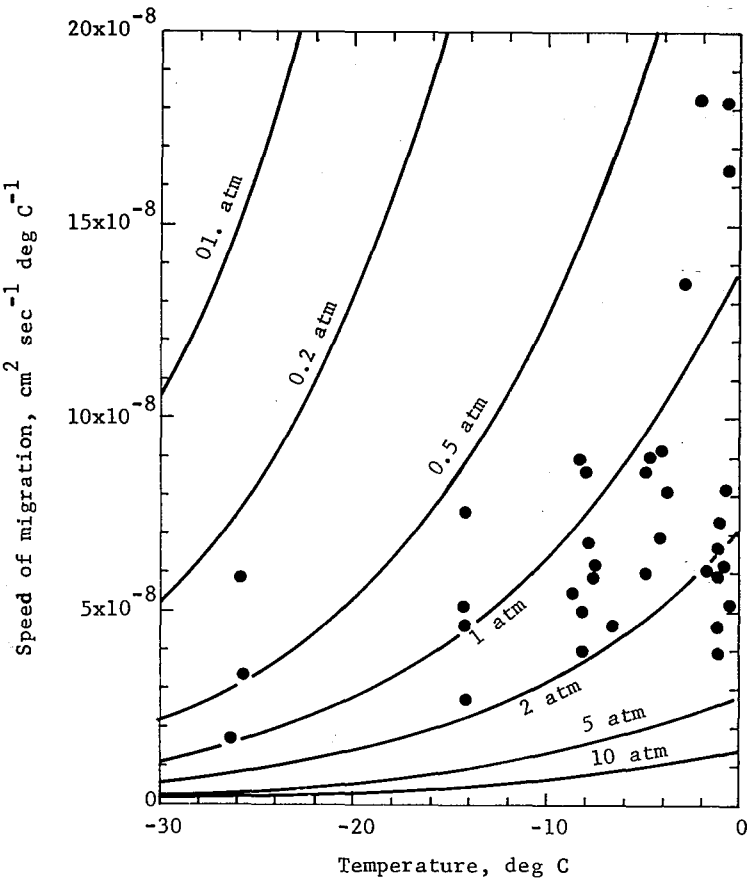

Fig. 2. Theoretical and observed velocities of approximately spherical bubbles. Solid lines are theoretical velocities at various air pressures

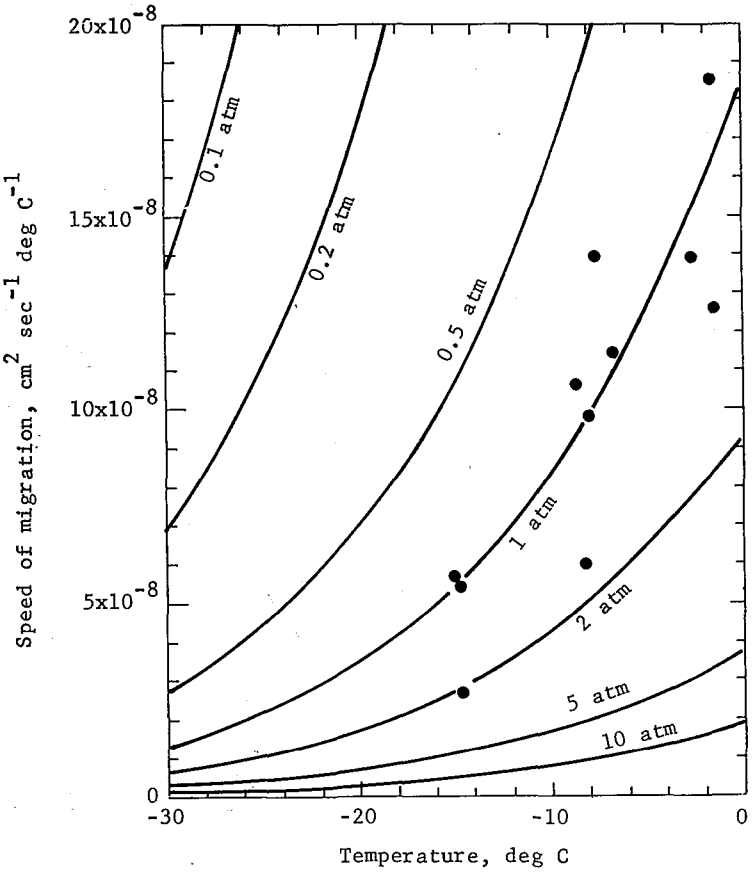

Fig. 3. Theoretical and observed velocities of circular cylindrical holes. Solid lines are theoretical velocities at various air pressures

The theoretical velocity of such a vapor figure, shown in Fig. 1, is, therefore, 14 % greater than the velocity calculated from Nakaya's formula.

The theoretical velocity of a spherical bubble is given by

$$\frac{1}{V} = \frac{1}{3}\frac{\rho\lambda}{K} + \frac{2}{3}\frac{\rho}{DC}, \tag{3}$$

and that of an infinitely long, right-circular cylindrical hole, the axis of which is perpendicular to the temperature gradient is given by

$$\frac{1}{V} = \frac{1}{2}\frac{\rho\lambda}{K} + \frac{1}{2}\frac{\rho}{DC}. \tag{4}$$

The velocities calculated from eqs. (3) and (4) are plotted in Figs. 2 and 3.

II. Experimental Study

Migration of air bubbles and vapor figures was observed at various temperatures and temperature gradients in 2.5- by 2- by 2-cm solid rectangular blocks of one or two

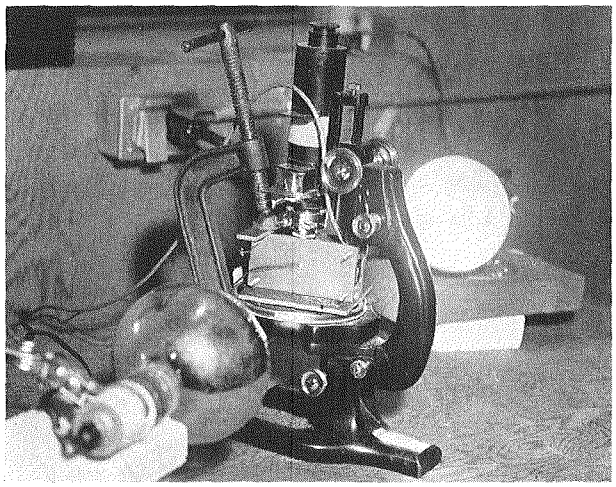

Fig. 4. Experimental setup, microscope and heat lamps

crystals of fresh-water ice. The ends of the blocks were frozen to copper plates maintained at different constant subfreezing temperatures by thermostatically controlled infrared lamps opposing the lower temperature of the cold room, which was regulated to within 2°C. The top, bottom, and sides of the blocks were insulated with 1 cm of rigid white polyurethane foam, the top piece being removed during observations. The positions of the bubbles or vapor figures were observed by means of a microscope equipped with a micrometer eyepiece. The experimental setup is illustrated in Fig. 4.

At the conclusion of observations, the specimen was removed from the apparatus, its dimensions were measured, and the orientation of the optic axis of the ice crystal with respect to the temperature gradient was determined.

Vapor figures. The succesive positions of vapor figures in which the temperature gradient was parallel to the *c*-axis were observed in five specimens. Neither a trend with time nor a limiting value of the velocity was observed, although Nakaya (1956, p. 33) concluded from similar observations that, with time, the vapor figure velocity approached a value of about 6.39 $cm \cdot sec^{-1} \cdot {}^{\circ}C^{-1} \cdot cm$.

In Fig. 1, the experimental and theoretical velocities of vapor figures determined in these experiments and in those of Nakaya (1956, pp. 32, 49) are plotted against the temperature at the figure. Because Nakaya did not report the temperature at the figure, the mean temperature of the specimen was used. The mean temperature was also used in some observations made in this investigation.

Air impedes diffusion of vapor across a vapor figure and, hence, diminishes the velocity of migration. The velocities of highly flattened oblate spheroidal vapor figures with $a/b = 0.1$ containing different air pressures were calculated from eq. (2) and the formula

$$D = D_0 \left(\frac{T}{T_0} \right)^m \frac{P_0}{P}, \tag{5}$$

(National Research Council, 1926, V. 5, p. 62) where $D_0 (=0.220)$ is the diffusion constant at $T_0 (=273°K)$ and $P_0 (=1$ atm), P is the pressure of the bubble, T is the temperature of the bubble, and $m (=1.75)$ is a constant.

All of the observed values lie below the theoretical velocity for the vapor figure with $a/b=0.1$, which is 14 % greater than the velocity given by Nakaya's formula. The influence of shape was observed in one specimen, in which a vapor figure became slightly thicker during migration and its velocity nearly doubled. Below a pressure of 10^{-2} atm, shape appears to be the dominant factor influencing the velocity.

The most likely explanation for the slowness of migration of many of the figures is probably that some air was present in them. The isopressure velocity curves (Fig. 1) show the large influence of a small air pressure on velocity. All but one of the observed points lie at a pressure below 0.2 atm, that is, above the 0.2-atm pressure line. Although no determination of air content of the vapor figures was made in this study, several bubble-free specimens from the same ice block as the test specimens were melted under kerosene, and were observed to contain air.

Air bubbles. The velocities of various shapes of air bubbles under temperature gradients were observed in eleven specimens. Both experimental and theoretical velocities of air bubbles are plotted against temperature at the bubble in Fig. 2 for the spherical bubbles, and in Fig. 3 for the cylindrical drilled holes. Although there is a great deal of scatter in each case, the observed velocities tend to support the theory. Velocity appears to be independent of the angle between the *c*-axis and the temperature gradient.

The primary influences on the migration velocity of air bubbles are shape, pressure and temperature. The influence of the ratio of polar to equatorial radii on the shape factors of eq. (2) was discussed earlier. In addition, the influence of shape is evident in the difference in theoretical velocities for spherical bubbles and cylindrical drilled holes (Figs. 2 and 3).

As the bubbles migrate, they become longer in the direction of migration, that is, the ratios a/b and m/n increase. The resulting decrease in A decreases the influence of diffusion in the bubble and increases the influence of conduction in the ice. At 1 atm, however, the convection term ρ/DC is at least ten times greater than the conduction term, except when A becomes very small.

The drilled holes, which were open to the atmosphere, migrated at velocities which lie with some scatter near the theoretical curve for 1 atm and which decrease with decreasing temperature. The initial increase in measured velocity corresponds to the increase in the ratio m/n; the final velocity measured, however, is, in most cases, less than the preceding one. This decrease may have been caused by the formation of frost in the holes or by development of very irregular shapes by the holes.

The scatter in the observed velocities of the cylindrical drilled holes is less than half that of the spherical bubbles although the change in polar and equatorial radii during migration was probably no greater for the spherical bubble. However, the greater the air pressure, the greater the impedance to the convection of water vapor across the bubble and, hence, the slower the velocity. The velocities of both spherical bubbles and cylindrical drilled holes containing air pressures greater and less than 1 atm were calculated using eqs. (3), (4) and (5).

Most of the specimens were obtained from commercial ice, which was frozen in 5-foot-deep tanks in which pressure ranges from 1.00 to 1.15 atm. In addition, a bubble formed near the center of the ice block in the final stages of freezing would be subjected

to an unknown increased pressure caused by the expansion of the ice in the process of freezing. These same specimens also contained numerous vapor figures since they had been subjected to solar radiation. The bubbles, therefore, could conceivably have had pressures anywhere from 1.15 atm for those which had formed near the bottom of the tank, to less than 1 atm for those which had merged with migrating vapor figure. The pressures of air bubbles in some specimens were measured and found to range from 0.44 to 1.5 atm. A bubble in one specimen, which increased in velocity from 0.9 time the theoretical velocity at 1 atm to 1.2 times it, at the same time exhibited a flat mirror-like hexagonal area on its warm wall. This may have been a vapor figure that the bubble encountered during migration, which decreased the air pressure, causing the velocity of the bubble to increase.

Frosting occurred in the interior of all air bubbles subjected to a temperature gradient except one, which apparently was not subjected to a large enough temperature gradient for a long enough time. No frosting was observed in bubbles not subjected to a temperature gradient. During migration under a temperature gradient, frost formed on the cold wall of the bubble (Figs. 5

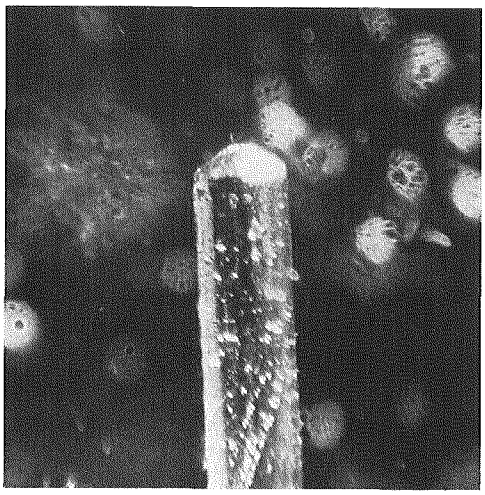

Fig. 5. Cylindrical drilled hole, 0.1 cm in diameter, before being subjected to a temperature gradient

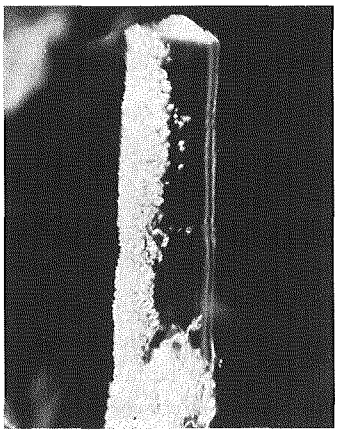

Fig. 6. Cylindrical drilled hole after 16 hours at a temperature of $-10°C$ with a $13.6°C \cdot cm^{-1}$ gradient parallel to the page and perpendicular to the axis, warm wall on left. Note frost formation on cold wall. Same scale as Fig. 5. The direction of migration was to the left

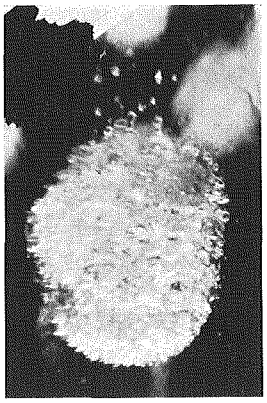

Fig. 7. Air bubble, about 0.25 cm in diameter, initially clear with $a/b=2/3$, after 100 hours at a temperature of $-14°C$ with a $21°C \cdot cm^{-1}$ gradient. Same direction of migration and orientation of gradient as in Fig. 6. Bump on warm wall formed during migration. Note irregular surface on cold wall where small bubbles have formed

and 6) as previously described by Nakaya (1956, p. 28). This frosting increased with time until the bubble was completely filled with frost (Fig. 7). At the same time, the walls of the frosted bubble became highly irregular. If migration of the bubble continued after the bubble completely frosted, the cold wall developed long, thin minute irregular fingering; whereas the warm wall developed larger, more irregular bumps. The fingering on the cold wall sometimes closed so that small bubbles were left behind (Fig. 7).

The reasons for frosting and its development are not entirely clear. In an air bubble with bumps on both the warm and cold walls, the lines of vapor diffusion would converge on the bump on the cold wall, causing it to grow faster than its surroundings, whereas the corresponding convergence at the bump on the warm wall would cause it to shrink. This would explain the presence of small fingering on the cold wall and no fingering on the warm wall; it fails, however, to explain the larger bumps on the warm wall. In addition, the same explanation would predict that a bump on the warm wall of a vapor figure would grow and one on the cold wall would shrink, whereas, no such irregularities were observed on the warm wall of vapor figures.

Several specimens were subjected to infrared irradiation at temperatures at or slightly below freezing. There was no noticeable change of the frost in the specimen below

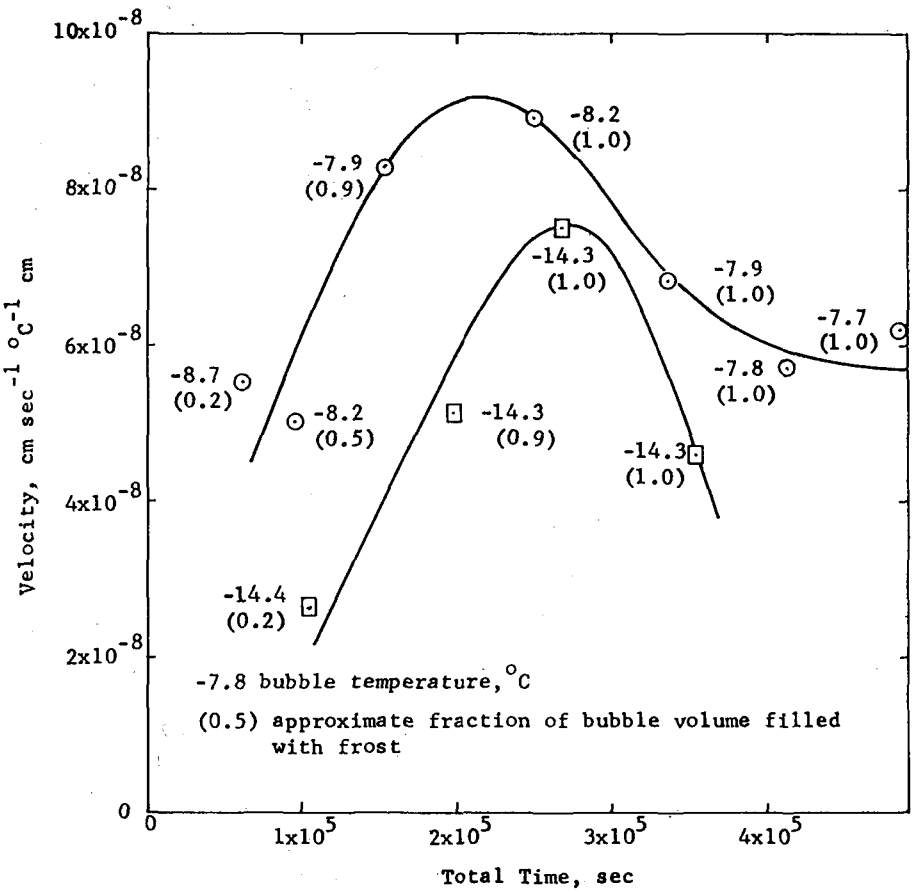

Fig. 8. Change in bubble velocity during frosting of two different specimens

zero after several hours of exposure, but in those at freezing, the frost appeared to melt and contract in area after several minutes of exposure, but did not disappear before the specimen melted a few minutes later. This indicates that, once formed at subfreezing temperatures, the frost does not readily disappear, even at the melting point.

The effect of frosting on the migration velocity of an air bubble is not readily apparent. Two bubbles at different gradients and temperatures were observed for several days after becoming completely frosted to note the effect of frost on the migration rate (Fig. 8). The velocities of both bubbles continued to increase for 19 hours after the bubbles were completely frosted, after which time, the velocity decreased to about 0.7 the maximum observed velocity.

The change in shape of the bubble during migration accounts for the initial increase in velocity of the bubble; the decrease in velocity may be due to development of the irregular shape after frosting or it may be due to the frost. It is not apparent in detail, however, how the frost or the irregular shape affect the rate of diffusion in order to decrease the velocity.

III. Summary

The results of this investigation substantiate those of Nakaya (1956), but do not support his theoretical formula for the migration velocities of vapor figures. The primary influences on the migration velocity of vapor figures are shape, internal air pressure, and temperature. Each of the observed figures has a shape such that the equatorial radius is less than about ten times the polar radius, which accounts for those observed velocities which exceed Nakaya's theoretical velocities. On the other hand, the presence of air in the vapor figures impedes the movement of water vapor across the figure which, in turn, decreases the migration velocity. Although Nakaya (1956, p. 13) has found little or no air in vapor figures, some figures in the ice used in this investigation did contain air.

The experimental results of this investigation support the theory put forth by Shreve for both vapor figures and air bubbles. In air bubbles as in vapor figures, shape, internal air pressure, and temperature influence velocity. During migration, the bubble elongates in the direction of migration; this change in the initial shape generally results in an increase in the velocity of migration. In addition, the bubbles have a measured pressure range of 0.44 to 1.5 atm, which would account for some of the scatter in velocities. The most striking example of the influence of air pressure on the migration velocity is the hundredfold difference in velocity between a bubble containing air at 1 atm and one containing no air. The influence of temperature is best demonstrated by the drilled holes, which migrated more slowly at lower temperatures.

A factor of undetermined importance is the formation of frost in bubbles during migration. Frost forms first on the cold wall, and then gradually fills the bubble. During frosting, the bubble changes to an irregular shape in which the warm wall develops large bumps, and the cold wall develops many small, thin irregular fingers, some of which are occasionally left behind as small bubbles. Once formed, the frost decreases but does not disappear even when the temperature is increased to the melting point. The effect of frost on the velocity is not apparent since frosted bubbles do not decrease in velocity

until 19 hours after they are completely frosted.

These experiments indicate that the migration velocity of an air bubble under a temperature gradient is too slow to account for the large occurrences of clear, bubble-free ice in temperate or polar glaciers unless some other, as yet unknown, mechanism becomes dominant as the melting temperature is approached. For example, a bubble at 1 atm in a temperate glacier under the normal pressure-melting temperature gradient of 6.6×10^{-6} °C·cm^{-1} would migrate at a velocity of 9.2×10^{-13} cm·sec^{-1} or 2.9×10^{-5} cm·yr^{-1}. A bubble in existence in a temperate glacier throughout the 3.5×10^{-4} years since the last major advance of continental glaciation would, therefore, have migrated only 1 cm, assuming it remained at the pressure melting temperature and 1 atm pressure.

In a polar glacier, the temperature gradient might be much greater since the ice 10 m below the surface is approximately at the mean annual surface temperature, whereas that at the bed of the glacier may be at the pressure melting temperature, although this is not known. A mean air temperature of −35°C would give a gradient of 3.4×10^{-4} °C·cm^{-1} in a 1 000-m-thick glacier, and a bubble velocity fifty times greater than that under the same conditions in a temperate glacier. Hence, a bubble at the pressure melting temperature and 1 atm in existence in the polar glacier since the last major advance of continental glaciation would have migrated 50 cm. Clearly, then, a much greater gradient is needed to account for the several-hundred-meter-long outcrops of bubble-free ice found in Antarctica.

Bubble migration under a temperature gradient, therefore, apparently cannot be called upon to account for the large occurrences of bubble-free ice in temperate and polar glaciers. In addition, from these experiments, it would appear that foliation is a passive structure within temperate glaciers, and that bubble migration under a temperature gradient does not account for the bubble-free layers in foliation in temperate glaciers. The larger temperature gradients in polar glaciers, however, could significantly modify foliation, which then would not lie passively within the ice.

In addition, there are other factors which may assist in the formation of foliation. In temperate glaciers, water is often observed in bubbles, which may increase the diffusion rate and, hence, the velocity. Clustering of the bubbles may be a self-perpetuating mechanism. A cluster of bubbles acts as an insulator so that the lines of heat flow diverge and the temperature gradient decreases at the bubbles. On approaching this smaller gradient, a bubble would decrease in velocity. Bubbles, therefore, would migrate from less to more bubbly areas.

References

1) ALLEN, C. R., KAMB, W. B., MEIER, M. F. and SHARP, R. P. 1960 Structure of the lower Blue Glacier, Washington. *J. Geol.*, **68**, 601–625.

2) ATHERTON, D. 1963 Comparisons of ogive systems under various regimes. *J. Glaciol.*, **4**, 547–557.

3) BADER, H. 1950 The Significance of air bubbles in glacier ice. *J. Glaciol.*, **1**, 443–451.

4) BARNES, H. T. 1928 Ice Engineering, Renouf Publishing Co., Montreal, 364 pp.

5) BUTKOVICH, T. R. 1953 Density of single crystals of ice from a temperate glacier. *SIPRE*

Res. Paper, **7**, 7 pp.

6) CRARY, A. P. and WILSON, C. R. 1961 Formation of "blue" glacier ice by horizontal compressive forces. *J. Glaciol.*, **3**, 1045–1050.

7) DORSEY, N. E. 1940 Properties of Ordinary Water-substance, Reinhold Publishing Corp., New York, 673 pp.

8) FISHER, J. E. 1962 Ogives of the Forbes type on alpine glaciers and a study of their origins. *J. Glaciol.*, **4**, 53–61.

9) FLINT, R. F. 1947 Glacial Geology and the Pleistocene Epoch, John Wiley and Sons, Inc., New York, 589 pp.

10) HOEKSTRA, P., OSTERKAMP, T. E. and Weeks, W. F. 1965 The migration of liquid inclusions in single ice crystals. *J. Geophys. Res.*, **70**, 5035–5041.

11) KAMB, W. B. 1959 Ice peterofabric observations from Blue Glacier, Washington, in relation to theory and experiment. *J. Geophys. Res.*, **64**, 1891–1909.

12) KAMB, W. B. and SHREVE, R. L. 1963 Structure of ice at depth in a temperate glacier (Abstract). *Trans. Amer. Geophys. Union*, **44**, 103.

13) KING, C. A. M. and LEWIS, W. V. 1961 A tentative theory of ogive formation. *J. Glaciol.*, **3**, 913–939.

14) KINGERY, W. D. and GCODNOW, W. H. 1963 Brine migration in salt ice. *In* Ice and Snow (W. D. KINGERY, *ed.*), M. I. T, Press, Cambridge, Mass., 237–247.

15) MALMGREN, F. 1927 Properties of Sea-ice, John Griegs Boktrykkerim, A/S, Bergen, 67 pp.

16) MCCALL, J. C. 1952 The internal structure of a cirque glacier. *J. Glaciol.*, **2**, 122–130.

17) NAKAYA, U. 1956 Properties of single crystals of ice revealed by internal melting. *SIPRE Res. Rept.*, **13**, 80 pp.

18) National Research Council 1926 International Critical Tables of Numerical Data, Physics, Chemistry and Technology, McGraw Hill Book Co., Inc., New York, **8**.

19) NUTT, D. C. 1959 Recent studies of gases in glacier ice. *Polar Notes*, No. 1, 57–65.

20) RAUSCH, D. O. 1958 Ice tunnel, Tuto area, Greenlasd, 1956. *SIPRE Tech. Rept.*, **44**, 34 pp.

21) RIGSBY, G. P. 1955 Study of ice fabrics, Thule area, Greenland. *SIPRE Rept.*, **26**, 6 pp.

22) SELIGMAN, G. 1949 The growth of the glacier crystal. *J. Glaciol.*, **1**, 254–268.

23) WEEKS, W. F. 1958 The structure of sea ice: a progress report. *In* Arctic Sea Ice. *Nat. Acad. Sci.-Nat. Res. conncil U.S.A., Publ*, **598**, 96–98.

24) WHITMAN, W. G. 1926 Elimination of salt from sea-water. *Amer. J. Sci., Ser. 5*, **11**, 126–132.

25) ZUMBERGE, J. H., GIOVENETTO, M., KEHLE, R. and Reid, J. 1960 Deformation of the Ross Ice Shelf, near the Bay of Whales, Antarctica. *IGY Glaciol. Rept. Ser.*, No. 3, 148 pp.